

Topological Spin Texture in a Quantum Anomalous Hall Insulator

Jiansheng Wu,^{1,2} Jie Liu,¹ and Xiong-Jun Liu^{1,3,4,*}

¹*Department of Physics, Hong Kong University of Science and Technology, Clear Water Bay, Hong Kong, China*

²*Department of Physics, South University of Science and Technology of China, Shenzhen 518055, China*

³*International Center for Quantum Materials and School of Physics, Peking University, Beijing 100871, China*

⁴*Department of Physics, Massachusetts Institute of Technology, Cambridge, Massachusetts 02139, USA*

(Received 17 May 2014; published 26 September 2014)

The quantum anomalous Hall (QAH) effect has been recently discovered in an experiment using a thin-film topological insulator with ferromagnetic ordering and strong spin-orbit coupling. Here we investigate the spin degree of freedom of a QAH insulator and uncover the fundamental phenomenon that the edge states exhibit a topologically stable spin texture in the boundary when a chiral-like symmetry is present. This result shows that edge states are chiral in both the orbital and spin degrees of freedom, and the chiral edge spin texture corresponds to the bulk topological states of the QAH insulator. We also study the potential applications of the edge spin texture in designing topological-state-based spin devices, which might be applicable to future spintronic technologies.

DOI: 10.1103/PhysRevLett.113.136403

PACS numbers: 71.10.Pm, 73.50.-h, 73.63.-b

The discovery of the quantum Hall effect in the 1980s brought about a fundamental concept, the topological state of quantum matter, in condensed matter physics [1,2]. In the quantum Hall effect an external magnetic field drives the electrons to fill in discrete Landau levels. This leads to a gap in the two-dimensional (2D) bulk, while the boundary exhibits 1D chiral gapless edge states. The Hall conductance in the integer quantum Hall effect is quantized by Chern numbers, which are integers and characterize the topology of the system [3]. The topological interpretation of the quantized Hall conductance implies that to obtain a quantum Hall state does not necessitate an external magnetic field. The theoretical idea of a quantum Hall effect without Landau levels, i.e., the quantum anomalous Hall (QAH) effect, was first introduced by Haldane in a honeycomb lattice over two decades ago [4]. Recent interest in this topological state has been revived due to great developments in the time-reversal-invariant topological insulators [5,6], with many new theoretical proposals having been introduced [7–13]. Importantly, following the proposal in Ref. [10], the QAH state has been detected in a recent experiment using a ferromagnetic (FM) thin-film topological insulator by observing the quantized Hall conductance [14].

While in the QAH effect the spin is generically not conserved, the recent experimental realization based on strongly spin-orbit (SO) coupled materials [14] motivates us to explore the spin degree of freedom of such QAH insulators. We show surprisingly that the edge states exhibit topologically stable spin texture in the boundary when a chiral-like symmetry is present, and such chiral edge spin texture corresponds to the bulk topological states of the QAH insulator. The potential applications of the edge spin texture are studied.

The minimal model for the QAH insulator is described by a two-band Hamiltonian $H = \sum_{\mathbf{k}} \psi_{\mathbf{k}}^{\dagger} \mathcal{H}(\mathbf{k}) \psi_{\mathbf{k}}$, where the spin basis $\psi_{\mathbf{k}} = (c_{\mathbf{k}\uparrow}, c_{\mathbf{k}\downarrow})^T$. Around the Γ point $\mathcal{H}(\mathbf{k})$ takes the simple (2 + 1)D Dirac form

$$\mathcal{H}(\mathbf{k}) = \begin{bmatrix} m_z + 2B(k_x^2 + k_y^2) & 2A_1 k_y + i2A_2 k_x \\ 2A_1 k_y - i2A_2 k_x & -m_z - 2B(k_x^2 + k_y^2) \end{bmatrix}, \quad (1)$$

where for the realization with thin-film FM topological insulators [10,14] m_z depends on the Zeeman term induced by the FM order, the B term characterizes the hybridization between top and bottom thin-film surfaces, and $2A_{1,2}$ equal Fermi velocities of the surface Dirac cones of the parent topological insulator [15,16]. The QAH phase is obtained when $m_z B < 0$, with the Chern number $C_1 = \text{sgn}(m_z A_1 A_2)$ [10,17]. In the solid-state experiment, Cr-doped $(\text{Bi}_{1-x}\text{Sb}_x)_2\text{Te}_3$ was used to achieve the above Hamiltonian and the QAH phase [14]. On the other hand, this model can also be realized in a square optical lattice [18] with SO coupling generated based on cold atom experiments [19–22].

In the typical isotropic case $|A_1| = |A_2|$ a chiral-like symmetry $S = \sigma_{\vec{n}_1} \mathcal{M}_{\vec{n}_2}$ emerges in the Hamiltonian, with $\vec{n}_1 \perp \vec{n}_2$ being arbitrary 2D orthogonal unit vectors in the x - y plane. Here $\sigma_{\vec{n}_1}$ and $\mathcal{M}_{\vec{n}_2}$ represent the \vec{n}_1 component of the Pauli matrix acting on the spin space and the spatial reflection along the \vec{n}_2 direction, respectively. The symmetry transforms the fermion operators via $S(c_{\mathbf{k}s}, c_{\mathbf{k}s}^{\dagger})^T = (\sigma_{\vec{n}_2})_{ss'} (c_{\mathbf{k}'s'}, c_{\mathbf{k}'s'}^{\dagger})^T$, with $s = \uparrow, \downarrow$, and $\mathbf{k}' = (k_{n_1}, -k_{n_2})$. One can verify for the second quantization Hamiltonian that $SHS^{\dagger} = H$, while the first quantization Hamiltonian satisfies $S\mathcal{H}(\mathbf{k})S^{\dagger} = -\mathcal{H}(\mathbf{k})$. Consider two edges normal to the \vec{n}_1 axis and we can reexpress the Hamiltonian as a summation of the 1D Hamiltonian with

fixed momentum k_{n_2} along the edge: $H = \sum_{k_{n_2}} H_{1D}(k_{n_2})$, where

$$H_{1D}(k_{n_2}) = - \int dx_{n_1} \psi_{k_{n_2}, x_{n_1}}^\dagger \left\{ [2B\partial_{x_{n_1}}^2 + m(k_{n_2})]\sigma_z + iA_1\partial_{x_{n_1}}\sigma_{n_2} - A_2k_{n_2}\sigma_{n_1} \right\} \psi_{k_{n_2}, x_{n_1}} \quad (2)$$

with $m(k_{n_2}) = m_z + 2Bk_{n_2}^2$. The above 1D Hamiltonian satisfies $SH_{1D}(k_{n_2})S^\dagger = H_{1D}(-k_{n_2})$, from which we know that $H_{1D}(0)$ describes a 1D topological insulator with chiral symmetry, and its two end states (i.e., edge states with $k_{n_2} = 0$ of the 2D system) must be eigenstates of $\sigma_{\bar{n}_1}$, with the spin oppositely polarized in the opposite edges [23]. Furthermore, using the $\mathbf{k} \cdot \mathbf{p}$ theory one can expand the 1D edge Hamiltonian up to the leading order of momentum and confirm that the edge states with nonzero k_{n_2} are also eigenstates of $\sigma_{\bar{n}_1}$. This result can be generalized to the case with a generic closed boundary condition [24]. In particular, for a material with a circular boundary, we can rewrite the Hamiltonian in the polar coordinate (r, φ) system

$$\mathcal{H}(r, \varphi) = \left[2B \left(\frac{1}{r} \partial_r r \partial_r + \frac{1}{r^2} \partial_\varphi^2 \right) + m_z \right] \sigma_z + i \frac{2A_1}{r} \sigma_r \partial_\varphi - i 2A_2 \sigma_\varphi \partial_r, \quad (3)$$

where $\sigma_r = \cos \varphi \sigma_x + \sin \varphi \sigma_y$ and $\sigma_\varphi = \cos \varphi \sigma_y - \sin \varphi \sigma_x$. The edge state of the eigenenergy \mathcal{E}_m can be described by $|\Phi_m^{\text{edge}}(r, \varphi)\rangle = |\phi_m^{\text{edge}}(r, \varphi)\rangle e^{im\varphi}$, with m being an integer. It can be verified from the eigenequation that $S|\phi_m^{\text{edge}}(r, \varphi)\rangle = |\phi_{-m}^{\text{edge}}(r, -\varphi)\rangle$, where $S = \sigma_r \mathcal{M}_\varphi$ (see the Supplemental Material [24] for details). On the other hand, the mirror transformation sends $\mathcal{M}_\varphi |\phi_m^{\text{edge}}(r, \varphi)\rangle = |\phi_{-m}^{\text{edge}}(r, -\varphi)\rangle$. Together with the two relations we reach

$\sigma_r |\phi_m^{\text{edge}}(r, \varphi)\rangle = |\phi_m^{\text{edge}}(r, \varphi)\rangle$, which shows that all of the edge modes are eigenstates of σ_r and exhibit spin texture in the boundary.

The numerical results are shown in Fig. 1 with different signs of $A_{1,2}$, B , and m_z . We see that the spin of edge states is in-plane polarized, and varies one cycle following the 1D closed path of the boundary. This spin texture shows that the edge states are chiral in both the orbital and spin degrees of freedom. Interestingly, the spin chirality gives a quantized Berry phase for each edge mode after evolving one cycle along the boundary: $\gamma_C = \pm\pi$, and this defines a 1D winding number $\mathcal{N}_{1d} = \pm 1$, which can be verified to correspond to the bulk Chern invariant via $C_1 = \mathcal{N}_{1d} \text{sgn}(m_z)$. With fixed $\text{sgn}(m_z)$, changing the edge spin chirality reverses the Chern number of the QAH insulator, while varying both the spin chirality and $\text{sgn}(m_z)$ gives phases with the same C_1 [see, e.g., Figs. 1(a) and 1(f)]. In Fig. 1 the chiral spin texture and edge currents are shown in different parameter regimes, and with square [Figs. 1(a)–1(d)] and circular [Figs. 1(e)–1(h)] geometries, respectively.

The above study manifests an interesting correspondence between the nontrivial topologies exhibited in the bulk and the boundary. The bulk Chern number is a topological invariant of the first Brillouin zone, which is a 2D closed manifold in momentum space due to the band gap of the insulator [3]. However, the 1D boundary is a closed manifold in position space, but not in momentum space since the edge modes are gapless. Therefore, the 1D edge invariant \mathcal{N}_{1d} is obtained in real space rather than in \mathbf{k} space, and the topological edge spin textures can be recognized as 1D real-space topological states. Both the bulk and edge topological states are classified by integers Z . Note that a 1D topological state necessitates symmetry protection [25]. The correspondence between the bulk and

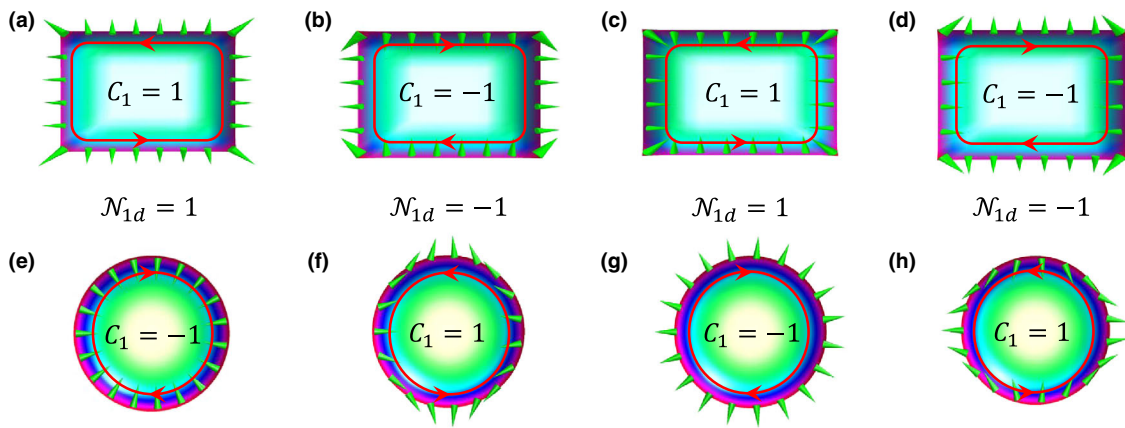


FIG. 1 (color online). (a)–(d) The edge spin texture for square geometry of the boundary, with the Zeeman term $m_z > 0$ and $B < 0$. (e)–(h), The edge spin texture for circular geometry of the boundary, with $m_z < 0$ and $B > 0$. For the other parameters, we take that $A_1, A_2 > 0$ (a), (e); $A_1 > 0, A_2 < 0$ (b), (f); $A_1, A_2 < 0$ (c), (g); and $A_1 < 0, A_2 > 0$ (d), (h). The topological spin textures give rise to quantized Berry phases if evolving the edge spin 1 circle along the boundary, which define 1D topological states in the position space of the boundary and are characterized by the 1D winding number \mathcal{N}_{1d} . The bulk Chern number C_1 corresponds to \mathcal{N}_{1d} with an additional sign factor $\text{sgn}(m_z)$.

edge topological phases relies on the chiral-like symmetry as introduced above, albeit the QAH insulator is an intrinsic topological state not depending on symmetry.

While the edge topological state is obtained under symmetry protection, the chirality enables the topological spin texture to be insensitive to local perturbations, which explicitly break the S symmetry. The local perturbation, which breaks this symmetry, includes the in-plane Zeeman fields, and the nonmagnetic and magnetic disorders. In the Supplemental Material [24] we show that the edge spin texture is not affected by the in-plane Zeeman fields without driving a topological phase transition in the bulk, and also is insensitive to the local disorder perturbations, even when the disorder strength is comparable with the bulk gap. Actually, just as the orbital chirality of the edge modes prohibits backscattering, the spin chirality ensures that no scattering occurs between two edge modes with opposite local spin polarizations. On the other hand, in the high-energy regime, due to the discrete lattice anisotropy the low-energy Hamiltonian may not apply. For the square lattice model the system only has S symmetry along the x and y directions. This ensures that the edge spin aligns along the x (y) axis in the edges normal to the \hat{e}_y (\hat{e}_x) direction and far away from the sample corners, while around the corners of the square sample the spin polarization of the high-energy edge modes may have a sizable tilt to the perpendicular direction [24].

The edge channel of the QAH insulator can be described by a 1D chiral Luttinger liquid [26,27]. Furthermore, the above study shows that the edge modes are chiral in both orbital and spin degrees of freedom. As the topological spin texture leads to quantized Berry phases, which can be integrated by Berry's connection, the edge states are governed by the following effective Hamiltonian

$$H_{\text{edge}} = iv_{\text{edge}} \int d\tilde{x} \psi_s^*(\tilde{x}) [\partial_{\tilde{x}} - i\mathcal{A}_s(\tilde{x})] \psi_s(\tilde{x}). \quad (4)$$

Here ψ_s denotes the orbital part of the edge states, \tilde{x} is the position parameter along the edge, and the Berry connection $\mathcal{A}_s = i\hbar \langle \chi_s(\tilde{x}) | \partial_{\tilde{x}} | \chi_s(\tilde{x}) \rangle$, with $|\chi_s(\tilde{x})\rangle$ representing the polarized spin degree of freedom. The integral of \mathcal{A}_s along the 1D boundary gives $\oint d\tilde{x} \mathcal{A}_s(\tilde{x}) = \mathcal{N}_{1d}\pi$. The π -Berry phase is equivalent to a half magnetic flux quanta threading through the 2D sample and encircled by the edge. According to the study by Wilczek [28], a half quantum flux can lead to 1/2 fractionalization of the orbital angular momentum. As a result, for the 2D sample with circular geometry, the orbital angular momentum of the edge modes should be fractionalized as $l_z = m + \mathcal{N}_{1d}/2$, with m being integers. The fractionalization of the orbital angular momentum has an observable in the edge spectrum $\mathcal{E}_{l_z} = v_{\text{edge}} l_z R_{l_z}^{-1}$, with R_{l_z} the effective radius of the edge state wave function. Because of the 1/2 fractionalization no zero-energy (midgap) edge state exists, and therefore the

total number of edge states is even. However, threading an additional magnetic 1/2-flux quanta can exactly push one original state to zero energy, changing the total number of edge modes to be odd, which provides an observable for the 1/2 fractionalization of the orbital angular momentum.

The spin and orbital chirality make the edge of the QAH insulator an exotic 1D metal, which has no correspondence in conventional 1D materials. The topological spin texture of the edge modes may lead to strong spin-dependent effects as presented below, which on the one hand can provide new unambiguous verification of the QAH state in the experiment, and, on the other hand, are applicable to spintronics by designing topological spin devices [29]. As illustrated in Fig. 2(a), we attach two metallic leads to the QAH sample, with a normal lead strongly coupled to the left-hand edge and a FM lead weakly coupled to the right-hand edge. Because of the spin texture, the couplings between the sample edge and leads are fully spin selective, which can lead to strong anisotropic effects in the tunneling conductance when changing the direction of magnetization \vec{M}_{FM} in the FM lead. The tunneling transport is studied with the Landauer formalism with a square lattice tight-binding model whose low-energy limit gives Eq. (1). With the coupling to normal and FM leads, we determine the retarded Green's function of the QAH insulator by $G^R(\omega) = (\omega - H - \Sigma^R)^{-1}$, where H is the tight binding Hamiltonian of the QAH insulator [24], and Σ^R is the

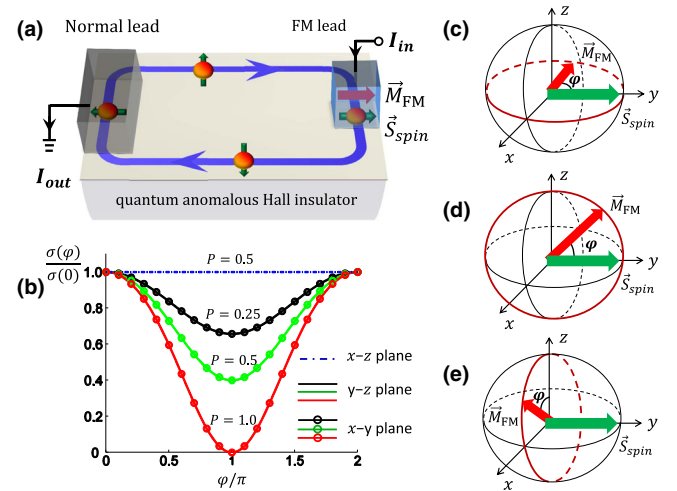


FIG. 2 (color online). (a) A normal metallic lead is strongly coupled to the left-hand edge and a FM lead is weakly coupled to the right-hand edge of the QAH insulator. Here the parameters for the quantum anomalous Hall phase satisfy $m_z > 0$, $A_{1,2} > 0$, and $B < 0$. Then the spin of the edge states in the right-hand edge points to the $+y$ direction. (b) The tunneling conductance $\sigma(\varphi)$ is plotted versus the azimuthal angle φ of the magnetization in the FM lead, with the magnetization varying in the x - y plane (c), y - z plane (d), and x - z plane (e), respectively. Numerical results are presented for different polarization ratios P in the FM lead. The maximum tunneling conductance is obtained when the magnetization aligns with the edge spin-polarization direction.

self-energy due to the couplings to the leads. Using the Fisher-Lee relation we can obtain the scattering matrix based on the Green's function and self-energies [30]

$$S_{p,q}^{ss'} = -\delta_{p,q}\delta_{\alpha\beta} + i[\Gamma_p^s]^{1/2}G_{s's'}^R[\Gamma_q^{s'}]^{1/2}. \quad (5)$$

Here, the matrix element $S_{p,q}^{ss'}$ ($s, s' = \uparrow, \downarrow$) denotes the scattering amplitude of the process where an electron is scattered from the spin state s' in lead q to the spin state s in lead p , with $p \neq q = L, R$ representing the left- and right-hand leads, respectively. $\Gamma_p^s = i[(\Sigma_p^{ss})^R - (\Sigma_p^{ss})^A]$, where $(\Sigma_p^{ss})^{R(A)}$ is the s -spin component retarded (advanced) self-energy due to the coupling to lead p . From the scattering matrix we obtain the tunneling conductance by $\sigma(\varphi) = (e^2/h)\sum_{s,s'}|S_{p,q}^{ss'}|^2$, where φ represents the direction of \vec{M}_{FM} in the FM lead.

The tunneling conductance $\sigma(\varphi)$ [Fig. 2(b)] exhibits a clear angle dependence when \vec{M}_{FM} varies in the x - y and y - z planes [Figs. 2(c) and 2(d)], while it is a constant when \vec{M}_{FM} varies along the x - z plane [Fig. 2(e)]. This measures that the edge spin polarizes to the y direction. The angle dependence implies a strong magnetoresistive effect by setting \vec{M}_{FM} along the $\pm y$ directions. The magnetoresistance, given by $\text{MR} = [\sigma(0) - \sigma(\pi)]/\sigma(\pi) \times 100\%$, is

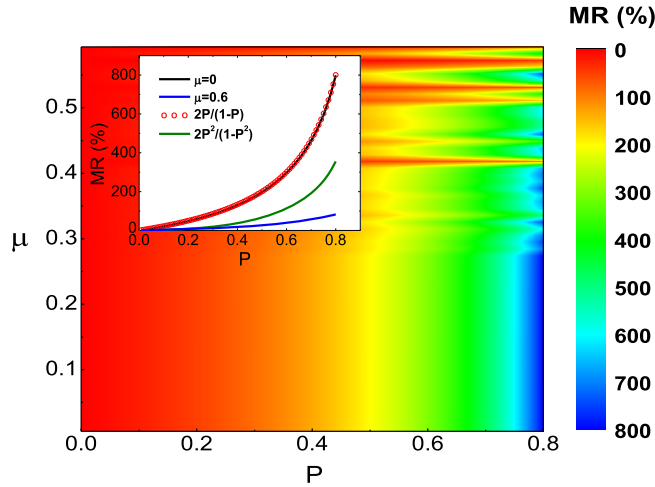


FIG. 3 (color online). Magnetoresistance for the setup in Fig. 2(a) by setting the magnetization of the FM lead along the $\pm y$ directions. The magnetoresistance (MR) is plotted numerically as a function of the polarization ratio P in the FM lead and the chemical potential μ (in units of B) in the QAH insulator. The parameters for the QAH phase are taken as $m_z = -0.3A_{1,2} = -0.3B$, which gives the bulk gap $E_g = 2|m_z| = 0.6B$. The MR is uniform versus μ when the chemical potential is within the bulk gap ($|\mu| < 0.3B$) and decreases when μ lies out of the gap. The inserted panel shows that the MR coincides with $2P/(1-P)$ for $|\mu| < 0.3B$ (black solid and red circled curves), which is significantly larger than the corresponding tunneling MR, given by $2P^2/(1-P^2)$ (green curve), in the conventional ferromagnet-insulator-ferromagnet devices with polarization ratio P in both ferromagnets [31].

plotted in Fig. 3 as a function of the chemical potential μ in the QAH insulator and the polarization ratio P of the FM lead. Because of the full spin polarization, the edge of the sample can be regarded as an ideal dissipationless half metal. This gives $\text{MR} \approx 2P/(1-P) \times 100\%$, which is significantly larger than the corresponding tunneling magnetoresistance obtained in conventional ferromagnet-insulator-ferromagnet devices with the same polarization ratio (the inserted panel of Fig. 3) [31]. The strong magnetoresistive effect has been widely applied to spintronics, especially to designing read heads [29].

Another interesting application of the topological spin texture is to design controllable spin-filtering devices, as illustrated in Fig. 4. The edge spin texture ensures that the

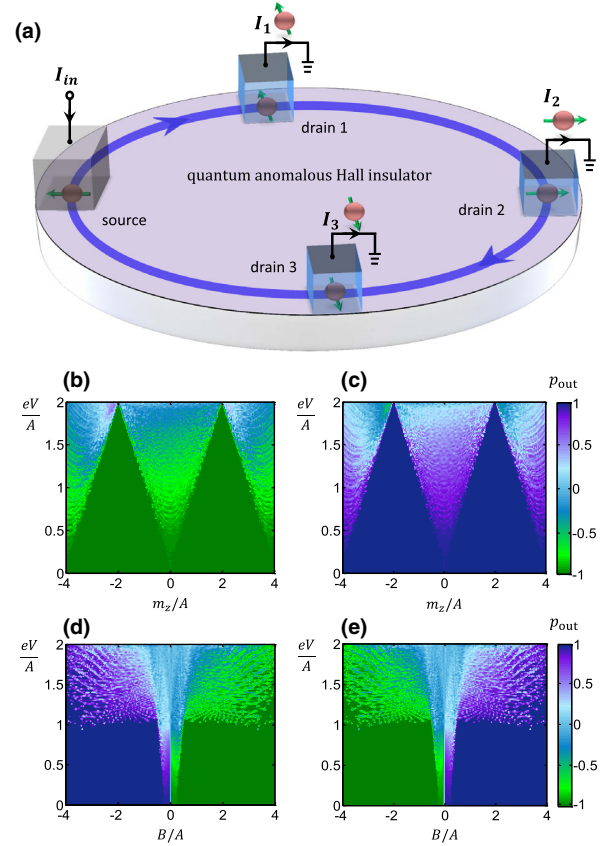


FIG. 4 (color online). Spin filtering effect and output spin-polarized current. (a) For a quantum anomalous Hall insulator with a circular boundary, the edge spin polarization depends on the direction of the 1D edge. This provides a controllable way to generate spin-polarized current by attaching normal-metal leads to different directions of the sample edge. (b)–(e) The polarization ratio p_{out} of the output spin current is plotted as a function of voltage eV in a drain lead and the Zeeman term m_z (b),(c) or B (d),(e), with the magnitudes rescaled by the SO coefficient A ($= |A_{1,2}|$). Other parameters are taken as $B = A_1 = A_2$ (a), $B = -A_1 = -A_2$ (b), $m_z = A_1 = A_2$ (c), and $m_z = -A_1 = -A_2$ (d). The sign change of p_{out} in (d) and (e) from the topological region with $B < 0$ to the region $B > 0$ implies that the edge spin reverses direction.

output current is fully spin polarized, with the polarization direction depending on which edge the drain lead is attached to. The spin-polarization ratio of the output current can be calculated from $p_{\text{out}} = \sum_s (|S_{p,q}^{s\uparrow}|^2 - |S_{p,q}^{s\downarrow}|^2) / \sum_{s,s'} |S_{p,q}^{ss'}|^2$. From the numerical results we see that when the voltage of the output lead lies in the sample bulk gap, the output current is 100% polarized to the same direction, reflecting that the spin texture is identical for all edge states. We note that the band gap of the currently realized QAH effect is small, while for realistic applications a larger topological gap is necessary. The new physics unveiled in this work and the proposed potential applications will motivate the search for new novel materials for QAH insulators with sizable band gaps in the future.

In conclusion, we have predicted that in SO coupled QAH insulators the edge states can exhibit topological spin textures in the boundary when a chiral-like symmetry is present, and have found that such topological spin textures have a correspondence to the bulk topological phases. We also studied the tunneling transport from a normal metal and FM leads to the chiral edge states and showed that the topological spin texture can induce strong magnetoresistance and spin filtering effects. These results may have potential applications in designing topological-state-based spin devices, which might be applicable to future spintronic technologies.

We thank K. T. Law for helpful comments. X.-J. L. also appreciates valuable discussions with Yayu Wang, Cenke Xu, Patrick A. Lee, Jairo Sinova, Zheng-Xin Liu, Meng Cheng, and X.-G. Wen. The authors thank the support of HKRGC through Grant No. 605512 and through Grant No. HKUST3/CRF/13G.

*Corresponding author.
xiongjunliu@pku.edu.cn

- [1] K. V. Klitzing, G. Dorda, and M. Pepper, *Phys. Rev. Lett.* **45**, 494 (1980).
- [2] D. C. Tsui, H. L. Stormer, and A. C. Gossard, *Phys. Rev. Lett.* **48**, 1559 (1982).
- [3] D. J. Thouless, M. Kohmoto, M. P. Nightingale, and M. den Nijs, *Phys. Rev. Lett.* **49**, 405 (1982).
- [4] F. D. M. Haldane, *Phys. Rev. Lett.* **61**, 2015 (1988).

- [5] M. Z. Hasan and C. L. Kane, *Rev. Mod. Phys.* **82**, 3045 (2010).
- [6] X.-L. Qi and S.-C. Zhang, *Rev. Mod. Phys.* **83**, 1057 (2011).
- [7] X.-L. Qi, Y.-S. Wu, and S.-C. Zhang, *Phys. Rev. B* **74**, 085308 (2006).
- [8] C.-X. Liu, X.-L. Qi, X. Dai, Z. Fang, and S.-C. Zhang, *Phys. Rev. Lett.* **101**, 146802 (2008).
- [9] C. Wu, *Phys. Rev. Lett.* **101**, 186807 (2008).
- [10] R. Yu, W. Zhang, H.-J. Zhang, S.-C. Zhang, X. Dai, and Z. Fang, *Science* **329**, 61 (2010).
- [11] X.-J. Liu, X. Liu, C. Wu, and J. Sinova, *Phys. Rev. A* **81**, 033622 (2010).
- [12] K. Nomura and N. Nagaosa, *Phys. Rev. Lett.* **106**, 166802 (2011).
- [13] X. Liu, H.-C. Hsu, and C.-X. Liu, *Phys. Rev. Lett.* **111**, 086802 (2013).
- [14] C.-Z. Chang *et al.*, *Science* **340**, 167 (2013).
- [15] H. Zhang, C.-X. Liu, X.-L. Qi, X. Dai, Z. Fang, and S.-C. Zhang, *Nat. Phys.* **5**, 438 (2009).
- [16] Y. Xia *et al.*, *Nat. Phys.* **5**, 398 (2009).
- [17] X.-L. Qi, T. L. Hughes, and S.-C. Zhang, *Phys. Rev. B* **78**, 195424 (2008).
- [18] X.-J. Liu, K. T. Law, and T. K. Ng, *Phys. Rev. Lett.* **112**, 086401 (2014).
- [19] X.-J. Liu, M. F. Borunda, X. Liu, and J. Sinova, *Phys. Rev. Lett.* **102**, 046402 (2009).
- [20] Y.-J. Lin, K. Jiménez-García, and I. B. Spielman, *Nature (London)* **471**, 83 (2011).
- [21] P. Wang, Z.-Q. Yu, Z. Fu, J. Miao, L. Huang, S. Chai, H. Zhai, and J. Zhang, *Phys. Rev. Lett.* **109**, 095301 (2012).
- [22] L. W. Cheuk, A. T. Sommer, Z. Hadzibabic, T. Yefsah, W. S. Bakr, and M. W. Zwierlein, *Phys. Rev. Lett.* **109**, 095302 (2012).
- [23] X.-J. Liu, Z.-X. Liu, and M. Cheng, *Phys. Rev. Lett.* **110**, 076401 (2013).
- [24] See Supplemental Material at <http://link.aps.org/supplemental/10.1103/PhysRevLett.113.136403> for more details.
- [25] A. P. Schnyder, S. Ryu, A. Furusaki, and A. W. W. Ludwig, *Phys. Rev. B* **78**, 195125 (2008).
- [26] B. I. Halperin, *Phys. Rev. B* **25**, 2185 (1982).
- [27] X.-G. Wen, *Phys. Rev. B* **41**, 12838 (1990).
- [28] F. Wilczek, *Phys. Rev. Lett.* **48**, 1144 (1982).
- [29] I. Žutić, J. Fabian, and S. Das Sarma, *Rev. Mod. Phys.* **76**, 323 (2004).
- [30] D. S. Fisher and P. A. Lee, *Phys. Rev. B* **23**, 6851 (1981).
- [31] M. Julliere, *Phys. Lett.* **54**, 225 (1975).